DISCRETE AND CONTINUOUS
DYNAMICAL SYSTEMS SERIES B
Volume **22**, Number **3**, May **2017**

doi:10.3934/dcdsb.2017050

pp. **1001–1021**

GLOBAL DYNAMICS OF A MODEL OF JOINT HORMONE TREATMENT WITH DENDRITIC CELL VACCINE FOR PROSTATE CANCER

Erica M. Rutter* and Yang Kuang

School of Mathematical & Statistical Sciences
Arizona State University
Tempe, AZ 85281, USA

Abstract. Advanced prostate cancer is often treated by androgen deprivation therapy, which is initially effective but gives rise to fatal treatment-resistant cancer. Intermittent androgen deprivation therapy improves the quality of life of patients and may delay resistance towards treatment. Immunotherapy alters the bodies immune system to help fight cancer and has proven effective in certain types of cancer. We propose a model incorporating androgen deprivation therapy (intermittent and continual) in conjunction with dendritic cell vaccine immunotherapy. Simulations are run to determine the sensitivity of cancer growth to dendritic cell vaccine therapy administration schedule. We consider the limiting case where dendritic cells are administered continuously and perform analysis on the full model and the limiting cases of the model to determine necessary conditions for global stability of cancer eradication.

1. **Introduction.** Prostate cancer is one of the most ubiquitous cancers in males in the United States, with an expected one in six men diagnosed in their lifetime [23]. The prostate requires androgens, especially testosterone and 5α-dihydrotestosteron (DHT) to function and continue proliferation. The current treatment protocol is to suppress androgen, which should lead to inhibited growth of cancer cells as well. However, although the initial response rates to therapy are excellent, eventually androgen independent prostate cancer arises and is most often fatal [33].

Recent research and clinical trials have begun to question whether the efficacy and comfort of this treatment could be increased by intermittent androgen deprivation (IAD) therapy [6, 22, 28, 37]. Intermittent androgen deprivation therapy works by administering androgen deprivation therapy until the patient reaches a certain threshold of prostate specific antigen (PSA), which is a biomarker of the disease. Upon reaching this threshold, the patient is removed from therapy until their PSA levels rise above a second threshold, when they are once again put on androgen deprivation therapy. This treatment still results in overall androgen suppression and may improve the quality of life of the individual patient, lessening the unpleasant side effects of androgen deprivation therapy [5, 18]. Although it has often been proposed that intermittent androgen deprivation therapy may increase time to androgen independent relapse, this statement remains unproven in clinical trials,

2010 *Mathematics Subject Classification.* Primary: 92C50, 34D20; Secondary: 34D23.

Key words and phrases. Mathematical modeling, prostate cancer, androgen deprivation therapy, immunotherapy, dendritic cell vaccine.

* The corresponding author.

including meta-studies [2, 5, 39, 43]. Of course, there are studies which suggest that only certain patient groups may benefit from intermittent androgen deprivation therapy, but determining those groups remains a work in progress [25, 44]. Adding to the confusion is the fact that there is no consensus in the medical community on the duration or intervals of the treatment [10]. Some have concluded that the findings determining that intermittent androgen deprivation therapy is non-inferior to continual androgen deprivation therapy are inconclusive due to flawed or inconsistent studies [17, 34].

Immunotherapy treatments use the body's immune system to fight against cancer by enhancing or repressing an immune response in the patient. Dendritic cells are the strongest of the antigen-presenting cells, meaning they ingest antigens and present the antigen material to naive and memory T cells in the system. These T cells then target the specific antigen for removal. Dendritic cell vaccines are created by extracting dendritic cells from the patient, loading the cells with antigens and re-injecting the dendritic cells into the patient. The target antigen in this case is PAP (Prostatic acid phosphatase), which has been used in clinical trials [3, 9, 40]. The dendritic cells then serve to activate the T cells into an immune response against PAP. Dendritic cell vaccines have been suggested as a method to improve the efficacy of hormone therapy treatment of advanced prostate cancer. In fact, Provenge is an FDA-approved dendritic cell vaccine for advanced prostate cancer which has been shown to extend the life of patients [4, 11].

An emerging field among mathematical oncology is determining optimal dosing strategies in order to manage cancer. Metronomic therapy, or the use of much lower dosages of medication more frequently, has been mathematically investigated as a possible alternative to large dosage strategies [29, 30]. There are many advantages towards this type of approach: lowering cytotoxicity, lowering costs, and increasing time until treatment resistance. This strategy aims to manage cancer, rather than eradicate it.

This research examines the effect of varying the frequency in which the patient receives dendritic cell vaccines on long term behavior of prostate cancer. We examine not only the case of discrete injections, but also consider a continuous injection, as through an intravenous (IV) therapy. We perform analysis on the model to determine biologically realistic parameter values which could result in stable condition of the disease or the elimination of the prostate cancer, and analytical results are corroborated with simulations. The parameters which do not have existing literature values, or are patient-specific, are thoroughly investigated with simulations to determine what changes to dendritic cell vaccine therapy must be implemented to delay the onset of androgen independent prostate cancer. Additionally, we examine the quasi-steady state system and perform a full analysis of the steady states, determining what conditions are necessary to generate global stability.

2. **Model formulation.**

There have been many mathematical models that discuss the evolution and treatment of prostate cancer using androgen deprivation therapy. In 2004, Jackson [20] formulated a partial differential equation model which featured both androgen independent and androgen dependent cancer cells. This model exhibited the effects of androgen independent relapse consistent with experimental data [20]. Ideta et. al [19] formulated a mathematical model comprised of ordinary differential equations designed to determine prostate cancer growth while on intermittent androgen therapy. Their model featured androgen concentration, androgen

independent, and androgen dependent cancer cells, with a term to model the mutation rate from androgen dependent to androgen independent in the absence of androgen.

Many have extended upon the model proposed by Ideta et. al. Hirata et. al [15] extended their model to include two sub-classes of androgen independent cancer cells: a subpopulation whose mutation to androgen independent was reversible, and a subpopulation who's mutation to androgen independent was irreversible. From this model, they have investigated how to optimize patient treatment protocols [14, 16]. Additionally, they were able to use the model to classify patients and determine whether intermittent androgen deprivation therapy would be more or less effective for each type of patient [13]. Most recently, they have analyzed their model to find conditions for existence non-trivial periodic orbits for one of the types of patients [12].

Tanaka et. al [41] extended the Ideta et. al model by incorporating stochasticity, for more realistic PSA level data. Portz et. al [37] introduced cell quotas to model how dependent the androgen dependent and androgen independent cancer cells are on androgen concentration. This model has been furthered by other researchers and compared to previous models [8, 32].

Immunotherapy has also been formulated by mathematicians. Kirschner and Panetta [24] established a model which quantified the anti-tumor immune response using populations of T cells, IL2, and tumor cells. Their model also allowed for incorporation of therapy. In the context of prostate cancer, Kronik et. al [26] formulated a mathematical model which investigated the response of prostate cancer to dendritic cell vaccines, corroborated with patient data. However, they only considered one type of tumor cell population and did not account for hormonal therapy.

There has been little work in investigating the combination of dendritic cell vaccines with any type of androgen deprivation therapy. Portz and Kuang [27, 36] examined immunotherapy in conjunction with IAD for prostate cancer which combined the Ideta et. al model [19] with the Kirschner and Panetta [24] model. Their system of 6 equations included androgen independent cells, androgen dependent cells, androgen, cytokines (IL-2), activated T cells, and dendritic cells. Recently, Peng et. al [35] used a 10-dimensional ordinary differential equation model to investigate how androgen deprivation therapy combines with immunotherapy, including dendritic cell vaccines. They were able to determine how to synergistically combine ADT with immunotherapy and fit their model with mouse data. However, their model did not take into account intermittent androgen deprivation therapy.

Our model is based on the Portz and Kuang [27, 36] model described above with some appropriate modifications. Their results showed that adding dendritic cell vaccines resulted in an increase in time to androgen independent relapse. However, the study did not consider how the dynamics of dosage amounts and frequencies for the dendritic cell vaccines might influence the outcome of the treatment. It has been hypothesized in a mathematical model that changing the dosages and frequency of administration of the dendritic cell vaccine may drastically alter the time to androgen independent relapse [26].

Our mathematical model is a population-style model of the interaction between androgen dependent cancer cells (X_1), androgen independent cancer cells (X_2), activated T cells (T), concentration of cytokine IL-2 (I_L), concentration of androgen

(A), and number of dendritic cells (D).

$$\frac{dX_1}{dt} = \underbrace{r_1(A,X_1,X_2)X_1}_{\text{growth and death}} - \underbrace{m_1(A)X_1}_{\text{mutation to AI}} + \underbrace{m_2(A)X_2}_{\text{mutation from AI}} - X_1 \underbrace{f_1(X_1,X_2,T)}_{\text{death by T cell}}, \quad (1)$$

$$\frac{dX_2}{dt} = \underbrace{r_2(X_1,X_2)X_2}_{\text{growth and death}} + \underbrace{m_1(A)X_1}_{\text{mutation from AD}} - \underbrace{m_2(A)X_2}_{\text{mutation to AD}} - X_2 \underbrace{f_2(X_1,X_2,T)}_{\text{death by T cell}}, \quad (2)$$

$$\frac{dT}{dt} = \underbrace{\frac{eD}{g+D}}_{\text{activation of T cell by DC}} - \underbrace{\mu T}_{\text{death}} + \underbrace{Tf_3(I_L,T)}_{\text{activation of T cell by cytokines}}, \quad (3)$$

$$\frac{dI_L}{dt} = \underbrace{Tf_4(X_1,X_2)}_{\text{secretion by tumor}} - \underbrace{\omega I_L}_{\text{degradation}}, \quad (4)$$

$$\frac{dA}{dt} = \underbrace{\gamma(a_0 - A)}_{\text{homeostasis of androgen}} - \underbrace{\gamma a_0 u(t)}_{\text{depletion of androgen if on therapy}}, \quad (5)$$

$$\frac{dD}{dt} = -\underbrace{cD}_{\text{death}}. \quad (6)$$

The androgen dependent cancer cells (AD) are governed by their proliferation and death (given by $r_1(A,X_1,X_2)$), their mutation to androgen independent cancer cells (AI), the mutation from androgen independent cells, and the number killed by T cells. The AI cancer cells are also governed by proliferation and death, independent of androgen, their mutation from AD cells, their mutation to AD cells, and the number killed by the T cells. The T cell counts are determined by the number activated by the dendritic cells, their natural death, and clonal expansion. The concentration of cytokines is determined by their production by stimulated T cells and a clearance rate. The concentration of androgen in the blood is described by homeostasis term and deprivation therapy term. The dendritic cells are governed by their death rate.

The modeling of the intermittent androgen deprivation therapy is governed by the $u(t)$. Note that if $u(t) = 1$, we are modeling the 'on-treatment' portion of the therapy, and when $u(t) = 0$, we model the 'off-treatment' therapy. Below are the detailed equations:

$$y(t) = c_1X_1 + c_2X_2, \quad (7)$$

$$u(t) = \begin{cases} 0 \to 1 & \text{if } y(t) > L_1 \text{ and } \frac{dy}{dt} > 0, \\ 1 \to 0 & \text{if } y(t) < L_0 \text{ and } \frac{dy}{dt} < 0. \end{cases} \quad (8)$$

In this case, $y(t)$ represents the serum PSA level. When the PSA level decreases below a certain threshold, L_0, the androgen deprivation therapy begins. When the PSA level increases above another threshold level, L_1, the 'on-treatment' therapy starts. Note that $L_0 < L_1$.

Although our model is similar to the Portz and Kuang model, we include three major changes which allow for a more realistic model. Firstly, we change the growth and death functions. The original model incorporated an exponential growth rate for the androgen independent cell population, which is very unrealistic. We modified this growth function to be logistic. Similarly, we change the growth and death for the androgen dependent cell population. We assume that the lack of androgen affects the androgen dependent cell population in two ways: lack of androgen lowers the

growth rate, and the lack of androgen actively kills the cell population. This is a realistic assumption which has been used in other prostate cancer models with great success [7,21]. We note that when androgen is at its homeostatic level, a_0, the growth rate of androgen dependent cells is at its highest. As the levels of androgen decrease, the growth rate of androgen dependent cells also decreases, and the death due to lack of androgen increases. When androgen is at its lowest value, 0, there is no growth of androgen dependent cells, and the highest death rate due to lack of androgen happens.

$$\begin{aligned} r_1(A, X_1, X_2) &= r_1 A \left(1 - \frac{X_1 + X_2}{K}\right) - \frac{d_1}{a_0}(a_0 - A), \\ r_2(X_1, X_2) &= r_2 \left(1 - \frac{X_1 + X_2}{K}\right). \end{aligned} \tag{9}$$

The second major change considers the mutation functions. The original model assumed that AD cells mutated to AI cells in an androgen-depleted environment. However, they did not consider the option that AI cells might mutate back to AD cells in an androgen-rich environment. We include this second mutation term in our model. If $A = a_0$, we note that there would be no mutation from AD to AI cell population, as we are at the homeostatic androgen levels. As we decrease the level of androgen, we increase the rate at which AD to AI mutations occur, until we reach $A = 0$, which gives the largest mutation rate m_1. For mutation from AI to AD, we assume a similar, but opposite function. When we have low levels of androgen, we assume that there is no mutation from AI to AD. However, as we increase through androgen levels, the mutation rate from AI to AD increases accordingly. The mutation rate functions are listed below.

$$\begin{aligned} m_1(A) &= m_1 \left(1 - \frac{A}{a_0}\right), \\ m_2(A) &= m_2 \left(\frac{A}{A + k_4}\right). \end{aligned} \tag{10}$$

The third major change we consider is using a generic class of functions for the four immune system interactions. As the immune system is extremely complicated with many interacting cells, there is not much data to help form a hypothesis on how these various components of the immune system interact together. In order to combat this, we consider functions that are generic, but we do want some basic properties for these functions. Specifically, we assume the following.

(A1): $f_1(X_1, X_2, 0) = f_2(X_1, X_2, 0) = f_3(0, T) = f_4(0, 0) = 0.$

(A2): $\dfrac{\partial f_1}{\partial X_1} \leq 0, \ \dfrac{\partial f_2}{\partial X_2} \leq 0,$ and $\dfrac{\partial f_1}{\partial T} \geq 0, \ \dfrac{\partial f_2}{\partial T} \geq 0.$

(A3): $\dfrac{\partial f_3}{\partial I_L} \geq 0, \ \dfrac{\partial f_4}{\partial X_i} \geq 0, \ i = 1, 2.$

3. **Simulations and observations.** There are many potential functions which could be excellent candidates for our f_i, but a logical choice would be a Holling Type II function. It is reasonable to assume that after a large enough presence of cancer cells, the death rate would approach a maximum death rate. It is not sensible to use a linear function which would assume the death rate is proportional to the

number of cancer cells. The functions that we propose and use for simulations are:

$$\begin{aligned} f_1(X_1, X_2, T) &= \frac{e_1 T}{g_1 + X_1 + X_2}, \\ f_2(X_1, X_2, T) &= \frac{e_2 T}{g_2 + X_1 + X_2}, \\ f_3(I_L, T) &= \frac{e_3 I_L}{g_3 + I_L}, \\ f_4(X_1, X_2) &= \frac{e_4(X_1 + X_2)}{g_4 + X_1 + X_2}. \end{aligned} \tag{11}$$

Explanations for the various parameters and their chosen values , as well as their respective sources are displayed in Table 1.

As we were unable to find a literature estimate on what the carrying capacity of the tumor cells would be, we decided to estimate with a brief calculation. The mean weight of a male prostate is 11 grams (7-16 grams) and the average human cell has a mass of 1 ng. Thus, we can conjecture that the carrying capacity is on the order of 10 billion cells.

In previous iterations of the immunotherapy mathematical model, hypothetical vaccines were administered every 30 days consisting of 0.3 million dendritic cells. In order to preserve the correct dosage, when the length between vaccinations was altered, the dosage was also altered accordingly. For the discrete case, variances from daily vaccinations to vaccinations separated by 120 days were considered. Simulations are extended to 4000 days to be able to determine long-term behavior of the prostate cancer. A continuous dose of dendritic cell vaccines was also considered, as if constantly administered through an IV. All simulations have the same initial conditions with initial AD count of 15 million cells, AI count of 0.1 million cells, 0 activated T cells, 0 concentration of cytokines (ng/mL) , 30 nmol/mL concentration of androgen, 0 dendritic cells. We have set the threshold to turn off treatment L_0 as 5 and the threshold to begin treatment L_1 as 15 $\frac{ng}{mL}$.

Once graphical results are obtained, it is advantageous to determine numerically and analytically whether the more successful dendritic cell vaccination timings have an overall effect.

3.1. **Discrete case.** For all numerics, we consider that $e_1 = e_2$, which means that T cells are able to kill AD and AI cancer cells equivalently. We begin by keeping $e_1 = e_2$, the effectiveness with which the T-cells eliminate cancer cells steady at a value of 0.75, which is reasonable within the range given in Table 1. We run a series of simulations, out to 4000 days, varying only the dosage level and frequency of the dendritic cell vaccine. The vaccination frequencies are varied from daily vaccinations to 120 days between each injection, and the dosages are varied from 0.01 to 1.20 million cells, respectively.

Figure 1 displays the PSA levels, androgen dependent (X_1) and androgen independent (X_2) cell densities versus time in days. We can see from the graph that the androgen suppression is triggered when the level reaches about 15 $\frac{ng}{mL}$, and is discontinued when the level reaches about 5 $\frac{ng}{mL}$. As can be seen, the PSA levels eventually skyrocket, indicating rise of androgen independent cancer. When the PSA levels grow drastically, it is clear that androgen suppression therapy is no longer effective. The effect is clear in the corresponding AD and AI graphs: the AD cancer cells are eliminated in the infrequent injections, which gives rise to the

P	Biological Meaning	Value	Source
r_1	AD cell proliferation rate	0.025/day	[1]
d_1	AD cell death rate	0.064/day	[1]
K	cancer cell carrying capacity	11 billion	
k_4	AI to AD mutation half-saturation	1.7	
r_2	AI net cell growth rate	0.006/day	[1]
m_1	maximum mutation rate from AD to AI	0.00005/day	[19]
m_2	maximum mutation rate from AI to AD	0.00015/day	[37]
a_0	base level androgen concentration	30 ng/ml	[19]
γ	androgen clearance and production rate	0.08/day	[19]
ω	cytokine clearance rate	10/day	[38]
μ	T cell death rate	0.03//day	[24]
c	dendritic cell death rate	0.14/day	[31]
e_1	max rate T cells kill AD cancer cells	0-1/day	[24]
g_1	AD cancer cell saturation level for T cell kill rate	10 x 10^9 cells	[24]
e_2	max rate T cells kill AI cancer cells	0-1/day	[24]
g_2	AI cancer cell saturation level for T cell kill rate	10 x 10^9 cells	[24]
e	T cell max activation rate	20 x 10^6 cells/day	[24]
g	DC saturation level for T cell activation	400 x 10^6 cells	[40]
e_3	max clonal expansion rate	0.1245/day	[24]
g_3	IL-2 saturation level for T cell clonal expansion	1000 ng/ml	[24]
e_4	max rate T cells produce IL-2	5 x 10^{-6} ng/ml/cell/day	[24]
g_4	cancer cell saturation level for T cell stimulation	10 x 10^9 cells	[24]
D_1	DC vaccine dosage	300 x 10^6 cells	[40]
c_1	AD cell PSA level correlation	1 x 10^{-9} ng/ml/cell	[19]
c_2	AI cell PSA level correlation	1 x 10^{-9} ng/ml/cell	[19]

TABLE 1. Values of parameters (P), explanations, and cited sources of every parameter used in this mathematical model.

more fatal androgen independent cancer. This is exhibited through the AI count, which skyrockets in the infrequent injection case. The rapid increase of AI cells indicates that the more fatal androgen resistant prostate cancer has begun. From these graphs, it is apparent that more frequent injections of the dendritic cell vaccine can help the effectiveness of the intermittent hormone therapy, delaying the rise of androgen independent cancer.

We can see that by increasing the frequency of the injections, but keeping the total dosage identical, there are vast improvements in the survival time of the patient. In order to quantify this relationship, we perform numerical analysis to determine the lowest value of e_1 required for the solution to produce a limit cycle. A limit

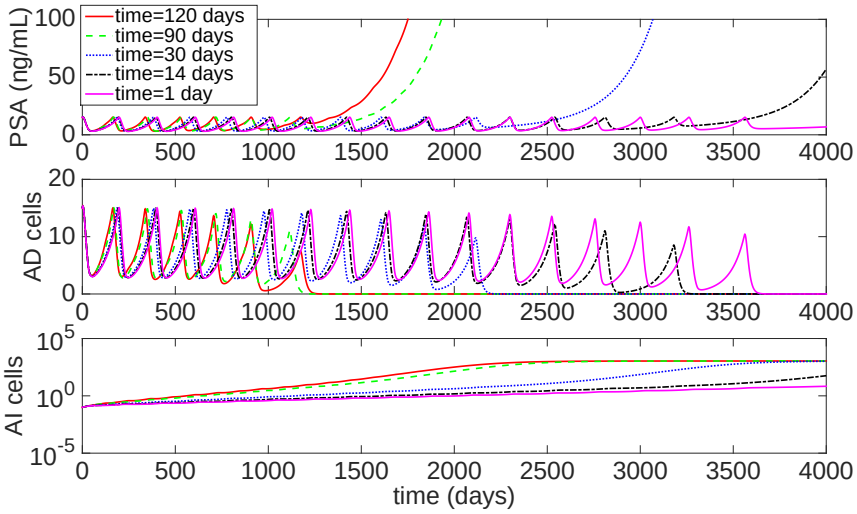

FIGURE 1. PSA serum concentration, androgen dependent (AD), and androgen independent (AI) cell concentrations for various dendritic cell vaccine injection times with an $e_1 = e_2$ of 0.75. More frequent injections result delay of the rise of fatal androgen independent cancer.

cycle in this case would represent a stable disease equilibrium, where the cancer is indefinitely responsive to IAD treatment. Recall that e_1, e_2 represent the cytotoxicity of the T-cells, a measure of how efficient a T cells is at killing the tumor cells. The biological range, as stated in 1 ranges from 0-1, cancer cells killed per day. A summary of the limit cyclical behavior is charted in figure 2.

We immediately notice that as vaccine timing is shortened, the minimal value of e_1 necessary to exhibit a stable disease state also decreases. We recall that e_1 could be a patient-specific parameter, as it is the maximum rate that T cells kill cancer cells per day. Thus, for those with weaker immune systems, more frequent injections could be much more effective. We note that for cases where the vaccine timing is greater than 30 days, even with values of maximal $e_1 = 1$, there is no stable disease state. Therefore, infrequent large doses of vaccine are much less effective at stabilizing the disease. Additionally, we can examine the shape of the limit cycles: as we increase the frequency of the dosage, we notice that the limit cycles are much smoother.

3.2. **Continuous case.** We have shown that, even for total amount of vaccine being constant, more frequent dendritic cell vaccine administrations are more effective than infrequent administrations. If we consider the limiting case of this behavior, we arrive at the case of a continual injection, as if the patient is always connected to the vaccine through an IV system. In order to accommodate for the continual injection, we slightly modify the equation (6) representing the dendritic cell numbers to: $\frac{dD}{dt} = v - cD$, where v is the continual injection rate.

The simulation begins in this case with an initial injection of 0.04 billion dendritic cells, which is then kept constant throughout the duration of the simulation. For this

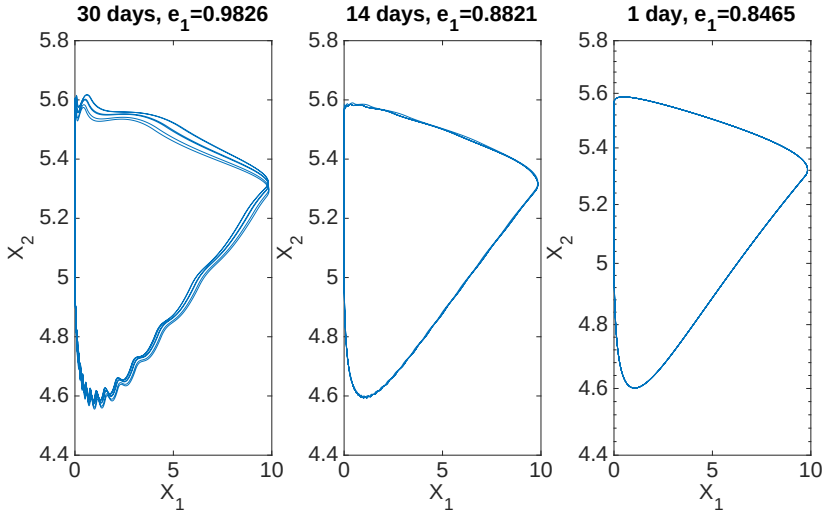

FIGURE 2. Limit cycle solutions for androgen dependent X_1, and androgen independent X_2 cancer cells. The minimal value of e_1 required to produce limit cycle behavior is noted above each solution. As vaccine timing decreases, minimal e_1 necessary to have stable disease state decreases.

continuous case, a variety of values of e_1 were considered, to determine if continuous vaccinations may help eliminate cancer. Figure 3 displays the PSA concentration for the different cases. We can see that contrary to the discrete case, it is apparent that even at lower values of $e_1 = 0.25$, the cancer is manageable. In fact, we even see elimination of cancer for very large values of e_1, for $e_1 > 0.75$.

In order to clearly see if the cancer is manageable for lower values of e_1 we turn to the cell counts for AD and AI cancer cells. Figure 3 displays these counts for the continual dendritic cell vaccinations. It is apparent for the duration of the simulation, AI cells only become dominant for the e_1 values of 0 and 0.25. This implies that androgen independent cancer is avoidable for a larger range of e_1 values than in the discrete case. This means that despite a weaker auto-immune response, it may be possible to suppress the growth of androgen independent cancer cells. Additionally, the treatment cycle lengths are very different depending on the e_1 value: as we increase through our e_1 value, we see that the length of 'off-treatment' is much longer, resulting in more comfort for the patient.

Since we see a full range of behavior as we increase through e_1, we take a closer look at a bifurcation diagram for the parameter. The resulting bifurcation diagram is shown in Figure 4. We can see that during most biologically relevant parameter values of e_1, which is a range of 0-1, we have cyclical behavior. At the smallest range of $e_1 = 0$, we have stability of carrying capacity equilibrium. However, once we increase past $e_1 = 0$, we can see that we have stable cyclical behavior. As observed in Figure 3, as we increase through e_1 we continue observing stable disease cycles. Finally, for higher values of e_1, we notice that the cycles collapse into a single steady state solution, which is stable. As we continue increasing e_1 past this point, the steady state approaches zero, which represents the eradication of the disease. We note that in examining the solutions for small values of e_1, the

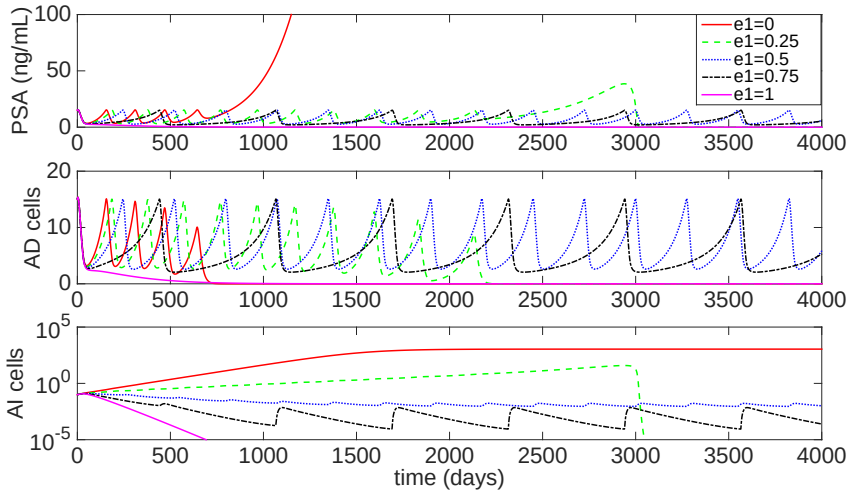

FIGURE 3. PSA serum level, AD cell density, and AI cell density for continual dendritic cell vaccinations, with an injection rate 0.04 billion cells for various values of e_1. It is apparent that in this continuous case, a wider range of e_1 is able to suppress the growth of cancer and elongate the cycles of IAD.

graph appears to be zigzagging. We believe this may be due to the model dynamics having a long transition time before approaching the limiting periodic state. We also have interesting dynamics at $e_1 = 0.24$, where we seem to approach a steady state, before the solution switches back into cyclical behavior.

4. **Basic properties of the system.** Although numerically studying the behavior of equations is useful, further information can be gathered by analysis of the equations themselves. It is also a metric to ensure that the behavior of the solutions have biological meaning. In order to analyze our equations, we assume that we are in fact continuously suppressing the androgen, instead of intermittent suppression. This assumption will lead to the following change of equation governing the concentration of androgen:

$$\frac{dX_1}{dt} = r_1(A, X_1, X_2)X_1 - m_1(A)X_1 + m_2(A)X_2 - X_1 f_1(X_1, X_2, T), \tag{12}$$

$$\frac{dX_2}{dt} = r_2(X_1, X_2)X_2 + m_1(A)X_1 - m_2(A)X_2 - X_2 f_2(X_1, X_2, T), \tag{13}$$

$$\frac{dT}{dt} = \frac{eD}{g + D} - \mu T + T f_3(I_L, T), \tag{14}$$

$$\frac{dI_L}{dt} = T f_4(X_1, X_2) - \omega I_L, \tag{15}$$

$$\frac{dA}{dt} = -\gamma A, \tag{16}$$

$$\frac{dD}{dt} = v - cD. \tag{17}$$

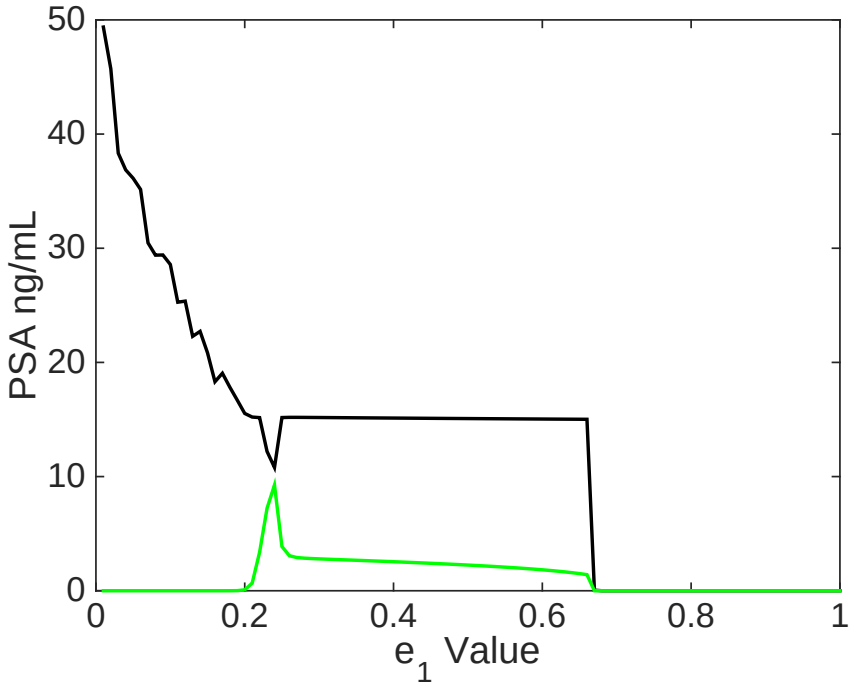

FIGURE 4. Birfurcation digram for parameter e_1, a measure of cytotoxicity of T-cells. Maximum PSA level in black, minimum PSA level in green. Carrying capacity is stable only for $e_1 = 0$. Immediately after, we have a Hopf bifurcaton and limit cycles, until we reach $e_1 \approx 0.66$, after which the disease-free steady state is stable.

Proposition 1. *Solutions of* (12)-(17) *that start positive remain positive.*

Proof. Solutions for D and A are explicitly solvable, whose solutions are positive. If solutions do not remain positive there must be some time $t_1 > 0$ such that $X_1(t_1) = 0$, $X_2(t_1) = 0$, $T(t_1) = 0$ or $I_L(t_1) = 0$. We examine the first case where $X_1(t_1) = 0$. Then $X_1'(t) \geq -m_1(A)X_1, \quad \forall\ t \in [0, t_1]$, or more specifically, $X_1(t_1) \geq X_1(0)e^{-m_1(A)t_1} > 0$, which is a contradiction. Similar arguments can be extended to the remaining variables, ensuring positivity of all solutions. □

We now examine the equations in detail to determine equilibrium points and their respective stabilities. We hope that this will give us as sense of biological meaning. What values must biological parameters exhibit in order for prostate cancer to be eliminated?

Proposition 2. *The model system* (12)-(17) *has a disease-free equilibrium* $E_0^* = (0, 0, \frac{ev}{\mu(cg+v)}, 0, 0, \frac{v}{c})$ *with growth functions* (9)*, mutation functions* (10)*, and generic functions.* E_0^* *is unstable if* $r_2 > f_2(0, 0, T_0^*)$*, where* $T_0^* = \frac{ev}{\mu(cg+v)}$*, and locally asymptotically stable if* $r_2 \leq f_2(0, 0, T_0^*)$*. When* $r_2 > f_2(0, 0, T_0^*)$*, a positive endemic equilibrium* $E^* = (X_1^*, X_2^*, T^*, I_L^*, A^*, D^*)$ *emerges, stability unknown.*

Proof. All variables except X_2 are easily solved and have only one steady state. For X_2, we can either have $X_2^* = 0$, which exists always, or an X_2 that solves $g(X_2) := r_2 - \frac{r_2 X_2}{K} - f_2(0, X_2, T^*) = 0$. We examine this quantity in more detail by calculating its sign at $X_2 = 0$:

$$g(0) = r_2 - f_2(0, 0, T_0^*)$$

where $T_0^* = \frac{ev}{\mu(cg+v)}$ is the corresponding T^* value when $X_2^* = 0$. Next we calculate the sign as $X_2 \to K$, its maximum possible value:

$$g(K) = -f_2(0, K, T_K^*) < 0$$

Thus, if $r_2 - f_2(0, 0, T_0^*) < 0$, there is no biologically relevant X_2 value that solves $g(X_2^*) = 0$, since the function f_2 is monotonically decreasing in X_2. Therefore, there is only the trivial, disease-free equilibrium $E_0^* = (0, 0, \frac{ev}{\mu(cg+v)}, 0, 0, \frac{v}{c})$ in our domain.

On the other hand, if $r_2 - f_2(0, 0, T_0^*) > 0$ then, by the Intermediate Value Theorem, there must be some $X_2^* \in (0, K)$ which solves $g(X_2^*) = 0$, giving us an endemic equilibrium $E_1^* = (0, X_2^*, T_1^*, I_{L1}^*, 0, \frac{v}{c})$, representing androgen independent relapse.

Now that the equilibria have been found, we now turn to finding the eigenvalues of the Jacobian to determine stability. We examine the disease-free equilibrium E_0^*, which generates the following matrix:

$$\begin{pmatrix} a_{1,1} & 0 & 0 & 0 & 0 & 0 \\ m_1 & r_2 - f_2(0,0,T_0^*) & 0 & 0 & 0 & 0 \\ 0 & 0 & -\mu & T_0^* \frac{\partial}{\partial I_L} f_3(0, T_0^*) & 0 & \frac{ceg}{cg+v} \\ T_0^* \frac{\partial}{\partial X_1} f_4(0,0) & T_0^* \frac{\partial}{\partial X_2} f_4(0,0) & 0 & -\omega & 0 & 0 \\ 0 & 0 & 0 & 0 & -\gamma & 0 \\ 0 & 0 & 0 & 0 & 0 & -c \end{pmatrix}$$

where $a_{1,1} = -d_1 a_0 - m_1 - f_1(0, 0, T_0^*)$. This Jacobian results in the following set of eigenvalues: $(-d_1 a_0 - m_1 - f_1(0, 0, T_0^*), r_2 - f_2(0, 0, T_0^*), -\mu, -\omega, -\gamma, -c)$. Since we know that all parameters are non-negative, and assuming that all parameters are in fact positive, we can see that all eigenvalues except one are guaranteed to be negative. Only $r_2 - f_2(0, 0, T_0^*)$ has the possibility to be negative, positive, or zero. If $r_2 - f_2(0, 0, T_0^*) < 0$, we in fact have the cancer-free equilibrium to be stable. Otherwise if $r_2 > f_2(0, 0, T_0^*)$, the cancer-free equilibrium is unstable. □

We would like to understand biologically what this means. We write our stability condition as $r_2 < f_2(0, 0, T_0^*)$: this means the maximal growth rate of androgen independent cells is less than the death rate of androgen independent cells due to T cells. We observe that since these functions are monotone, in the case of strictly monotone function, we can invert f_2 to find an equivalent condition that involves T_0^*. Recalling that $T_0^* = \frac{ev}{\mu(cg+v)}$, this means we can solve for an explicit solution involving v, our critical dosage parameter. Theoretically, if the remaining parameters could be measured for a patient, a critical dosage could be calculated. We note that if given patient specific parameters such as their individual T cell

efficiencies, we are able to calculate a necessary dose level to stabilize the disease-free equilibrium. In the context of our proposed simulation functions f_i, given in (11), our condition for stability becomes $v > \frac{cgg_2r_2\mu}{e_2e-g_2r_2\mu}$, which is indeed a critical dosage value.

5. **Global analysis of limiting system.** As the full system is difficult to perform analysis on, we consider the limiting systems by performing a quasi-steady state approximation. This can give insight into the biology. We begin by assuming quasi-steady states for androgen, cytokines, and dendritic cells. This is a reasonable assumption, since the time scales at which these processes occur is much shorter than that of the populations of cancer cells growing. Then, we use the results of Thieme [42] to examine the asymptotic behavior of the limiting system. We consider the system when androgen deprivation therapy is continual ($A = 0$). We will examine the case where androgen deprivation therapy is continually on thoroughly and determine necessary conditions of $f_i(X_1, X_2, T)$ to obtain global stability of eradication of prostate cancer and conditions for global stability of the diseased steady state.

We examine the case where androgen deprivation therapy is turned on ($A = 0$). We let I_L, D, and A go to quasi-steady state. We end up with the following set of equations:

$$\frac{dX_1}{dt} = -d_1a_0X_1 - m_1X_1 - X_1f_1(X_1, X_2, T), \tag{18}$$

$$\frac{dX_2}{dt} = r_2X_2\left(1 - \frac{X_1 + X_2}{K}\right) + m_1X_1 - X_2f_2(X_1, X_2, T), \tag{19}$$

$$\frac{dT}{dt} = \frac{eD}{g + D} - \mu T + Tf_3(I_L, T), \tag{20}$$

$$I_L = \frac{Tf_4(X_1, X_2)}{\omega}, \tag{21}$$

$$A = 0, \tag{22}$$

$$D = \frac{v}{c}. \tag{23}$$

Note that:

$$\begin{aligned} \frac{dX_1}{dt} &= X_1\left[-d_1a_0 - m_1 - f_1(X_1, X_2, T)\right] \\ &\leq X_1\left[-d_1a_0 - m_1\right] \\ &\leq -aX_1. \end{aligned} \tag{24}$$

It is apparent that $\lim_{t\to\infty} X_1(t) = 0$. Thus we can reduce the system to:

$$\begin{aligned} \frac{dX_2}{dt} &= r_2X_2\left(1 - \frac{X_2}{K}\right) - X_2f_2(0, X_2, T), \\ \frac{dT}{dt} &= \frac{eD}{g + D} - \mu T + Tf_3(I_L, T), \end{aligned} \tag{25}$$

which is defined on the subdomain $\bar{\Omega} = \{(X_2, T) : X_2 \geq 0, T \geq 0\}$ and is the limiting system of (18)-(23).

Before we begin the analysis of the system, we would like to ensure that the behavior of the quasi-steady state system is analogous to the full system. We must quantify what dynamics are preserved and eliminated by simplifying the system.

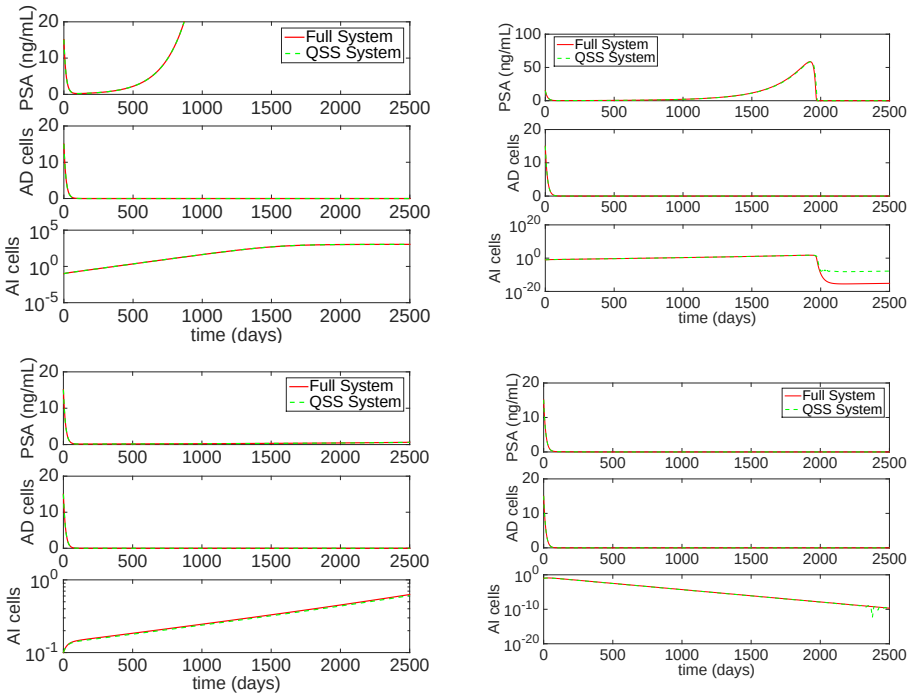

FIGURE 5. Comparisons of the full system and quasi-steady state system for various values of e_1: 0, 0.15, 0.25, and 0.65, assuming androgen deprivation therapy is constantly on. These values of e_1 show many differing dynamics. The quasi-steady state system closely approximates the full system in every case, but shows slight differences in the case of $e_1 = 0.15$

We run the system with the same parameters for the full system and for the reduced system. Figure 5 shows the comparison. We can see that by examining the quasi-steady state system we do lose some of the dynamics in certain cases, like when $e_1 = 0.15$. For all other values of e_1, however, we note that the quasi steady-sate system very closely resembles the full system, meaning that our results for the quasi-steady state system may be extended to the full system. We also note that our expected outcome – that X_1 goes to zero, is exhibited in all of the figures.

Theorem 5.1. *The disease-free steady state of* (18)-(23) *is globally asymptotically stable under the following conditions:*

i) $\mu > f_3(I_L, T)$,
ii) $r_2 < f_2(0, 0, T_0^*)$,
iii) $\frac{\mu^2(cg+v)}{ev} > \frac{\partial}{\partial T} f_3(0, T_0^*)$.

To prove this theorem, we break down the result into several propositions for simplicity. We will begin with positivity and boundedness, move to local asymptotic stability, and end with conditions necessary for global asymptotic stability.

Proposition 3. *If* $\mu > f_3(I_L, T)$ *then solutions of* (18)-(23) *remain positive and bounded.*

Proof. We begin with the proof for positivity, examining T first. We note that since we are assuming that $T(t_0) \geq 0$, in order for $T(t) < 0$ for some t, we would require that $\frac{dT}{dt} < 0$ when $T = 0$. However, $\frac{dT}{dt}|_{T=0} = \frac{eD}{g+D} > 0$ since all parameters are positive. For X_2, since we are assuming that $X_2(t_0) \geq 0$, in order for $X_2(t) < 0$ for some t, we would require that $\frac{dX_2}{dt} < 0$ when $X_2 = 0$. However, $\frac{dX_2}{dt}|_{X_2=0} = m_1 X_1 > 0$ since we have already proved that X_1 stays positive and all parameters are positive.

We have already proven that solutions remain nonnegative, so we now look to boundedness. We begin with T:

$$\begin{aligned} \frac{dT}{dt} &= \frac{eD}{g+D} + T(f_3(I_L, T) - \mu) \\ &\leq c - \bar{g}T \end{aligned} \tag{26}$$

where $\bar{g} = \min[\mu - f_3(I_L, T)] > 0$ by assumption. This implies that T is bounded.

We look towards the boundedness of X_2 now. We immediately see that X_2 is bounded above by K. □

Proposition 4. *The limiting system* (25) *contains two equilibria: the disease-free equilibrium and a negative equilibrium, under assumption ii): $r_2 < f_2(0, 0, T_0^*)$. The disease-free equilibrium is locally asymptotically stable under assumption ii) and iii): $\frac{g+D}{eD} > \frac{\partial}{\partial T} f_3(0, T_0^*)$.*

Proof. There are two possible equilibria of the system. Following the proof from Proposition 2: if $r_2 < f_2(0, 0, T_0^*)$, only the disease-free equilibrium exists, $E_0^* = (0, T_0^*)$. The local stability of the disease-free steady state $E_0^* = (0, \frac{ev}{\mu(cg+v)})$ is exhibited in the Jacobian:

$$\begin{pmatrix} r_2 - f_2(0, 0, T_0^*) & 0 \\ T_0^* \frac{\partial}{\partial X_2} f_3(0, T_0^*) & -\mu + T_0^* \frac{\partial}{\partial T} f_3(0, T_0^*) \end{pmatrix}$$

and the eigenvalues are given by $\lambda_1 = r_2 - f_2(0, 0, T_0^*) < 0$ as given by the assumptions, and $\lambda_2 = -\mu + T_0^* \frac{\partial}{\partial T} f_3(0, T_0^*) < 0$ (by condition iii), so we have local asymptotic stability. □

We are now ready to prove the main result for global asymptotic stability.

Proof of Theorem 5.1. Since solutions to the system are positive and bounded, we immediately see that there can be no limit cycles around our non-negative equilibrium, since our only equilibrium is on the boundary. By Poincare-Bendixson, all solutions tend towards the disease-free steady state, so E_0^* is globally asymptotically stable. □

We can interpret two of these conditions for the global stability in terms of biology. We can see that the condition $r_2 < f_2(0, 0, T_0^*)$ can be interpreted as the maximal intrinsic growth rate of the cancer cells must be less than the death rate due to the T cells. Recall that this was the condition for local stability of the full system, so we are unsurprised to see the same condition again. Similarly, $\mu > f_3(I_L, T)$ means that we want the death rate of the T cells to be greater than the production of T cells due to I_L. Now that we have examined the conditions for global stability for the disease-free equilibrium, we also want to explore the dynamics for the equilibrium that is not disease-free.

Theorem 5.2. *The diseased steady state of* (18)-(23) *is globally asymptotically stable under the following conditions:*

i) $\mu > f_3(I_L, T)$,
ii) $r_2 > f_2(0, 0, T_0^*)$,
iii) $\mu - f_3(I_L, T) > -X_2 \frac{\partial}{\partial X_2} f_2(X_1, X_2, T) + T \frac{\partial}{\partial T} f_3(I_L, T) - \frac{r_2 X_2}{K} \forall X_2, T \geq 0.$

To prove this theorem, we break down the result into several propositions for simplicity. We will begin with positivity and boundedness, move to local asymptotic stability, followed by eliminating limit cycles, and end with conditions necessary for global asymptotic stability.

Proposition 5. *If condition i) is satisfied, then solutions of* (18)-(23) *remain positive and bounded.*

Proof. Positivity and boundedness have already been proven in Proposition 3, and the results hold for current conditions, as long as we assume condition i). □

Proposition 6. *The limiting system* (25) *contains two equilibria: the disease-free equilibrium,* E_0^**, and a secondary equilibrium,* E_1^**. The secondary equilibrium is positive (assuming condition ii)). The disease-free equilibrium is a saddle point (under conditions ii) and iii)).*

Proof. The existence of the equilibria follow from Proposition 2, so we know that under condition ii), if $r_2 > f_2(0, T_0^*)$, we will have two biologically relevant equilibria: $E_0^* = (0, T_0^*) = (0, \frac{ev}{\mu(cg+v)})$ and $E_1^* = (X_2^*, T_1^*)$.

The local stability of the disease-free steady state E_0^* is exhibited in the Jacobian:

$$\begin{pmatrix} r_2 - f_2(0, T_0^*) & 0 \\ T_0^* \frac{\partial}{\partial X_2} f_3(0, T_0^*) & -\mu + T_0^* \frac{\partial}{\partial T} f_3(0, T_0^*) \end{pmatrix}$$

and the eigenvalues are given by $\lambda_1 = r_2 - f_2(0, T_0^*) > 0$ by condition ii) and $\lambda_2 = -\mu + T_0^* \frac{\partial}{\partial T} f_3(0, T_0^*) < 0$, by condition iii). Thus, the disease-free equilibrium is a saddle point.

Now we examine the Jacobian of the diseased equilibrium:

$$\begin{pmatrix} -\frac{r_2 X_2^*}{K} - X_2^* \frac{\partial}{\partial X_2} f_2(X_2^*, T_1^*) & -X_2^* \frac{\partial}{\partial T} f_2(X_2^*, T_1^*) \\ T_1^* \frac{\partial}{\partial X_2} f_3(I_L^*, T_1^*) & -\mu + T_1^* \frac{\partial}{\partial T} f_3(I_L^*, T_1^*) + f_3(I_L^*, T_1^*) \end{pmatrix}.$$

Thus, the trace is given by

$$\tau = -\frac{r_2 X_2^*}{K} - X_2^* \frac{\partial}{\partial X_2} f_2(X_2^*, T_1^*) - \mu + T_1^* \frac{\partial}{\partial T} f_3(I_L^*, T_1^*) + f_3(I_L^*, T_1^*) \tag{27}$$

and the determinant is given by

$$\begin{aligned} \Delta = &\left(-\frac{r_2 X_2^*}{K} - X_2^* \frac{\partial}{\partial X_2} f_2(X_2^*, T_1^*) \right) \left(-\mu + f_3(I_L, {}^* T_1^*) + T_1^* \frac{\partial}{\partial T} f_3(I_L^*, T_1^*) \right) \\ &+ \left(X_2^* \frac{\partial}{\partial T} f_2(X_2^*, T_1^*) T_1^* \frac{\partial}{\partial X_2} f_3(I_L^*, T_1^*) \right). \end{aligned} \tag{28}$$

In order for E_1^* to be stable we require $\tau < 0, \Delta > 0$. Notice that $\tau < 0$ is given by assuming condition iii). However, we have no idea about the sign of Δ. Given our information of $\tau < 0$, we know that E_1^* is either a saddle point or a stable node/spiral. □

Proposition 7. *The limiting system* (25) *has no limit cycles as long as condition iii) is satisfied.*

Proof. We will be using the Dulac criterion to establish that there are no periodic orbits within. Using $h(X_2, T) = \frac{1}{X_2}$, we can see that

$$\begin{aligned}\Delta &= \frac{\partial}{\partial X_2}\left[\frac{1}{X_2}\left(r_2 X_2\left(1-\frac{X_2}{K}\right) - X_2 f_2(X_2,T)\right)\right] \\ &\quad + \frac{\partial}{\partial T}\left[\frac{1}{X_2}\left(\frac{eD}{g+D} - \mu T + T f_3(I_L,T)\right)\right] \\ &= \frac{\partial}{\partial X_2}\left[r_2 - \frac{r_2 X_2}{K} - f_2(X_2,T)\right] + \frac{\partial}{\partial T}\left[\frac{eD}{X_2(g+D)} - \frac{\mu T}{X_2} + \frac{T(f_3(I_L,T))}{X_2}\right] \\ &= -\frac{r_2}{K} - \frac{\partial}{\partial X_2} f_2(X_2,T) - \frac{\mu}{X_2} + \frac{f_3(I_L,T)}{X_2} + \frac{T}{X_2}\frac{\partial}{\partial T} f_3(I_L,T)\end{aligned}$$

To ensure that there are no periodic orbits, we must prove that this quantity Δ does not change sign. We begin by re-writing this condition:

$$X_2\Delta = -\frac{r_2 X_2}{K} - X_2\frac{\partial}{\partial X_2} f_2(0,X_2,T) - \mu + f_3(I_L,T) + T\frac{\partial}{\partial T} f_3(I_L,T). \tag{29}$$

We know that for $X_2, T \geq 0$, $\Delta < 0$ by condition iii). Thus, the Dulac criterion has ensured that we will have no periodic orbits in our domain. □

We are now ready to prove the main result for global asymptotic stability.

Proof of Theorem 5.2. By Proposition 7, we can see that there are no limit cycles present. Solutions are positive and bounded, and the model system has two fixed points, one of which is a saddle point. By the Poincare-Bendixson theorem, we know that there are three possibilities: all solutions tends to a fixed point, all solutions tend to a periodic orbit, or there is a homoclinic or heteroclinic orbit which connects our two fixed points. We have ruled out periodic orbits by Dulac criterion using condition iii).

Now we must show there is no homoclinic or heteroclinic orbits connecting our fixed points.

In order to show there is no heteroclinic orbit connecting the two fixed points, we look towards the stable manifold of the saddle point. Looking back towards our Jacobian, we can clearly see that the stable manifold is given by the T-axis

$$\begin{pmatrix} X_2 \\ T \end{pmatrix} = \begin{pmatrix} 0 \\ 1 \end{pmatrix}. \tag{30}$$

Due to assumption ii), we notice that near the disease free steady state E_0^*, we have $dX_2(t)/dt > 0$. These observations preclude the existence of a heteroclinic orbit connecting E_0^* and E_1^*.

The fact that $dX_2(t)/dt > 0$ near E_0^* also implies that there is no homoclinic orbit originating from E_0^*. There can not be any homoclinic orbits originating from E_1^* if it is stable. The Dulac criteria also rules out homoclinic orbits originating from E_1^* if it is a saddle.

By Poincare-Bendixson Theorem, the only option remaining is that all solutions of (25) converge to E_1^*. Thus, E_1^* is globally asymptotically stable. □

6. **Conclusion.** Current treatment options for late-stage prostate cancer are suboptimal in terms of survival and quality of life. By examining a model of intermittent hormone therapy coupled with dendritic cell vaccines, we are able to prolong both the life and quality of life of the patient. We found that, keeping total yearly dosages the same, more frequent injections are conducive to managing prostate cancer for a longer period of time. We extrapolate this idea to the extreme by modifying the model to include a 'continual' dosage, as if administered through an intravenous fluid.

In our model, there are several parameters which are patient specific, or do not have accepted literature values. We examined the effect of varying values of e_1, the killing T-cell efficiency. Predictably, increasing e_1 led from androgen independent relapse, to stable limit cyclical behavior, and when increased enough, total eradication of the disease. This parameter measures how effective dendritic cell vaccine therapy will be - if e_1 is small, the therapy will be negligible. e_1 also acts to elongate the cycle times for a stable cyclical disease, which means increased time for the period when the patient is not undergoing androgen deprivation therapy. We performed bifurcation analysis on parameter e_1 to examine the various behaviors that exist in the system. As our simulations only considered the case where $e_1 = e_2$, we could also investigate how the dynamics change when we allow these values to be different.

Additionally, for mathematical analysis, we simplify the model to have continuous androgen suppression, in order to determine the effect of continual dosages. We notice there are two possible equilibria – cancer-free equilibrium and an androgen independent (fatal) cancer equilibrium. If our continual dosage is less than a determined critical value, the cancer-free equilibrium exists, but it is unstable. If our continual dosage is higher than that critical value, the cancer-free equilibrium is stable and a cancerous equilibrium is born (stability unknown). These findings have biological significance. In previous papers it has been determined that for a 30-day vaccine, it is necessary for a large values of e_1 to ensure cancer-free progression [36]. In this analysis, we could have smaller values of e_1 that still result in stable disease-free equilibrium. For patients with less effective immune systems (lower e_1 values), it is possible to eradicate cancer with higher presence of dendritic cells. As dendritic cell vaccines are not known to have an adverse effect on the human body, it is possible that for patients with weakened immune systems, a tailored dose could be administered.

We further examined the limiting cases of behavior for this system, by allowing several parameters to go to quasi-steady state. We were able to determine requirements for global stability – or the guarantee of elimination of prostate cancer in some cases. Additionally, we were able to determine further conditions for the global stability of the endemic equilibrium.

Despite the insights that this model has afforded us, there is still much to be done. Future work may include comparing the model with available patient data. This will allow us to determine the efficacy of this model at predicting behavior of the prostate cancer. We will also be able to explore the patient-specific parameters and the effect these have on final outcome. Additionally, we would like to be able to compare our model with other patient-data validated models. Mathematically, the

local stability of the endemic equilibrium of the full system should also be studied in detail.

Acknowledgments. EMR is partially supported by an ASU research grant and YK is partially supported by an NSF grant DMS 1518529. The authors would like to acknowledge Alex P. Farrell and Rebecca A. Everett for their comments and help. The authors also thank the valuable suggestions from the anonymous reviewer.

REFERENCES

[1] R. R. Berges, J. Vukanovic, J. I. Epstein, M. CarMichel, L. Cisek, D. E. Johnson, R. W. Veltri, P. C. Walsh and J. T. Isaacs, Implication of cell kinetic changes during the progression of human prostatic cancer, *Clinical Cancer Research*, **1** (1995), 473–480.

[2] T. E. A. Botrel, O. Clark, R. B. Dos Reis, A. C. L. Pompeo, U. Ferreira, M. V. Sadi and F. F. H. Bretas, Intermittent versus continuous androgen deprivation for locally advanced, recurrent or metastatic prostate cancer: A systematic review and meta-analysis, *BMC Urology*, **14** (2014), p9.

[3] P. A. Burch, G. A. Croghan, D. A. Gastineau, L. A. Jones, J. S. Kaur, J. W. Kylstra, R. L. Richardson, F. H. Valone and S. Vuk-Pavlović, Immunotherapy (apc8015, provenge®) targeting prostatic acid phosphatase can induce durable remission of metastatic androgen-independent prostate cancer: A phase 2 trial, *The Prostate*, **60** (2004), 197–204.

[4] M. A. Cheever and C. S. Higano, Provenge (sipuleucel-t) in prostate cancer: The first fda-approved therapeutic cancer vaccine, *Clinical Cancer Research*, **17** (2011), 3520–3526.

[5] J. M. Crook, C. J. O'Callaghan, G. Duncan, D. P. Dearnaley, C. S. Higano, E. M. Horwitz, E. Frymire, S. Malone, J. Chin and A. Nabid et al., Intermittent androgen suppression for rising psa level after radiotherapy, *New England Journal of Medicine*, **367** (2012), 895–903.

[6] J. M. Crook, E. Szumacher, S. Malone, S. Huan and R. Segal, Intermittent androgen suppression in the management of prostate cancer, *Urology*, **53** (1999), 530–534.

[7] S. Eikenberry, J. Nagy and Y. Kuang, The evolutionary impact of androgen levels on prostate cancer in a multi-scale mathematical model, *Biology Direct*, **5** (2010), 24–24.

[8] R. Everett, A. Packer and Y. Kuang, Can mathematical models predict the outcomes of prostate cancer patients undergoing intermittent androgen deprivation therapy?, *Research on the Physics of Cancer*, **9** (2016), 139–157.

[9] L. Fong, D. Brockstedt, C. Benike, J. K. Breen, G. Strang, C. L. Ruegg and E. G. Engleman, Dendritic cell-based xenoantigen vaccination for prostate cancer immunotherapy, *The Journal of Immunology*, **167** (2001), 7150–7156.

[10] M. Gleave, L. Klotz and S. S. Taneja, The continued debate: Intermittent vs. continuous hormonal ablation for metastatic prostate cancer, *Urologic Oncology: Seminars and Original Investigations*, **27** (2009), 81–86, Proceedings: Annual Meeting of the Society of Urologic Oncology/Society for Basic Urologic Research (May 2007).

[11] C. S. Higano, P. F. Schellhammer, E. J. Small, P. A. Burch, J. Nemunaitis, L. Yuh, N. Provost and M. W. Frohlich, Integrated data from 2 randomized, double-blind, placebo-controlled, phase 3 trials of active cellular immunotherapy with sipuleucel-t in advanced prostate cancer, *Cancer*, **115** (2009), 3670–3679.

[12] Y. Hirata and K. Aihara, Ability of intermittent androgen suppression to selectively create a non-trivial periodic orbit for a type of prostate cancer patients, *Journal of Theoretical Biology*, **384** (2015), 147–152.

[13] Y. Hirata, K. Akakura, C. S. Higano, N. Bruchovsky and K. Aihara, Quantitative mathematical modeling of psa dynamics of prostate cancer patients treated with intermittent androgen suppression, *Journal of Molecular Cell Biology*, **4** (2012), 127–132.

[14] Y. Hirata, S.-i. Azuma and K. Aihara, Model predictive control for optimally scheduling intermittent androgen suppression of prostate cancer, *Methods*, **67** (2014), 278–281.

[15] Y. Hirata, N. Bruchovsky and K. Aihara, Development of a mathematical model that predicts the outcome of hormone therapy for prostate cancer, *Journal of Theoretical Biology*, **264** (2010), 517–527.

[16] Y. Hirata, M. di Bernardo, N. Bruchovsky and K. Aihara, Hybrid optimal scheduling for intermittent androgen suppression of prostate cancer, *Chaos: An Interdisciplinary Journal of Nonlinear Science*, **20** (2010), 045125.

[17] M. Hussain, C. Tangen, C. Higano, N. Vogelzang and I. Thompson, Evaluating intermittent androgen-deprivation therapy phase iii clinical trials: The devil is in the details, *Journal of Clinical Oncology*, **34** (2016), 280–285.
[18] M. Hussain, C. M. Tangen, D. L. Berry, C. S. Higano, E. D. Crawford, G. Liu, G. Wilding, S. Prescott, S. Kanaga Sundaram and E. J. Small et al., Intermittent versus continuous androgen deprivation in prostate cancer, *New England Journal of Medicine*, **368** (2013), 1314–1325.
[19] A. M. Ideta, G. Tanaka, T. Takeuchi and K. Aihara, A mathematical model of intermittent androgen suppression for prostate cancer, *Journal of Nonlinear Science*, **18** (2008), 593–614.
[20] T. Jackson, A mathematical model of prostate tumor growth and androgen-independent relapse, *Discrete and Continuous Dynamical Systems - Series B*, **4** (2004), 187–201.
[21] H. V. Jain, S. K. Clinton, A. Bhinder and A. Friedman, Mathematical modeling of prostate cancer progression in response to androgen ablation therapy, *Proceedings of the National Academy of Sciences*, **108** (2011), 19701–19706.
[22] H. V. Jain and A. Friedman, Modeling prostate cancer response to continuous versus intermittent androgen ablation therapy, *Discrete and Continuous Dynamical Systems - Series B*, **18** (2013), 945–967.
[23] A. Jemal, R. Siegel, E. Ward, Y. Hao, J. Xu, T. Murray and M. J. Thun, Cancer statistics, *CA: A Cancer Journal for Clinicians*, **58** (2008), 71–96.
[24] D. Kirschner and J. C. Panetta, Modeling immunotherapy of the tumor–immune interaction, *Journal of Mathematical Biology*, **37** (1998), 235–252.
[25] L. Klotz and P. Toren, Androgen deprivation therapy in advanced prostate cancer: Is intermittent therapy the new standard of care?, *Current Oncology*, **19** (2012), S13–S21.
[26] N. Kronik, Y. Kogan, M. Elishmereni, K. Halevi-Tobias, S. Vuk-Pavlović and Z. Agur, Predicting outcomes of prostate cancer immunotherapy by personalized mathematical models, *PLoS One*, **5** (2010), e15482.
[27] Y. Kuang, J. D. Nagy and S. E. Eikenberry, *Introduction to Mathematical Oncology*, CRC Press, 2016.
[28] S. Larry Goldenberg, N. Bruchovsky, M. E. Gleave, L. D. Sullivan and K. Akakura, Intermittent androgen suppression in the treatment of prostate cancer: A preliminary report, *Urology*, **45** (1995), 839–845.
[29] U. Ledzewicz, M. Naghnaeian and H. Schättler, Optimal response to chemotherapy for a mathematical model of tumor–immune dynamics, *Journal of Mathematical Biology*, **64** (2012), 557–577.
[30] U. Ledzewicz and H. Schättler, Optimal bang-bang controls for a two-compartment model in cancer chemotherapy, *Journal of Optimization Theory and Applications*, **114** (2002), 609–637.
[31] M. T. Lotze and A. W. Thomson, *Dendritic Cells: Biology and Clinical Applications*, Access Online via Elsevier, 2001.
[32] J. D. Morken, A. Packer, R. A. Everett, J. D. Nagy and Y. Kuang, Mechanisms of resistance to intermittent androgen deprivation in patients with prostate cancer identified by a novel computational method, *Cancer Research*, **74** (2014), 3673–3683.
[33] P. S. Nelson, Molecular states underlying androgen receptor activation: A framework for therapeutics targeting androgen signaling in prostate cancer, *Journal of Clinical Oncology*, **30** (2012), 644–646.
[34] J. C. Park and M. A. Eisenberger, Intermittent androgen deprivation in prostate cancer: Are we ready to quit?, *Journal of Clinical Oncology*, **34** (2016), 211–214.
[35] H. Peng, W. Zhao, H. Tan, Z. Ji, J. Li, K. Li and X. Zhou, Prediction of treatment efficacy for prostate cancer using a mathematical model, *Scientific Reports*, **6** (2016), 21599.
[36] T. Portz and Y. Kuang, A mathematical model for the immunotherapy of advanced prostate cancer, in *BIOMAT 2012*, World Scientific, 2013, 70–85.
[37] T. Portz, Y. Kuang and J. D. Nagy, A clinical data validated mathematical model of prostate cancer growth under intermittent androgen suppression therapy, *AIP Advances*, **2** (2012), 011002.
[38] S. A. Rosenberg and M. T. Lotze, Cancer immunotherapy using interleukin-2 and interleukin-2-activated lymphocytes, *Annual Review of Immunology*, **4** (1986), 681–709.
[39] A. Sciarra, P. A. Abrahamsson, M. Brausi, M. Galsky, N. Mottet, O. Sartor, T. L. Tammela and F. C. da Silva, Intermittent androgen-deprivation therapy in prostate cancer: A critical review focused on phase 3 trials, *European Urology*, **64** (2013), 722–730.

[40] E. J. Small, P. Fratesi, D. M. Reese, G. Strang, R. Laus, M. V. Peshwa and F. H. Valone, Immunotherapy of hormone-refractory prostate cancer with antigen-loaded dendritic cells, *Journal of Clinical Oncology*, **18** (2000), 3894–3903.

[41] G. Tanaka, Y. Hirata, S. L. Goldenberg, N. Bruchovsky and K. Aihara, Mathematical modelling of prostate cancer growth and its application to hormone therapy, *Philosophical Transactions of the Royal Society of London A: Mathematical, Physical and Engineering Sciences*, **368** (2010), 5029–5044.

[42] H. R. Thieme, Convergence results and a poincaré-bendixson trichotomy for asymptotically autonomous differential equations, *Journal of Mathematical Biology*, **30** (1992), 755–763.

[43] H.-T. Tsai, D. F. Penson, K. H. Makambi, J. H. Lynch, S. K. Van Den Eeden and A. L. Potosky, Efficacy of intermittent androgen deprivation therapy vs conventional continuous androgen deprivation therapy for advanced prostate cancer: a meta-analysis, *Urology*, **82** (2013), 327–334.

[44] J. M. Wolff, P.-A. Abrahamsson, J. Irani and F. Calais da Silva, Is intermittent androgen-deprivation therapy beneficial for patients with advanced prostate cancer?, *BJU International*, **114** (2014), 476–483.

Received October 2015; revised April 2016.

E-mail address: Erica.Rutter@asu.edu
E-mail address: kuang@asu.edu